

# Tumor-suppressive effects of Smad-ubiquitination regulator 2 in papillary thyroid carcinoma

GUIRONG LUO<sup>1\*</sup>, LITING ZHANG<sup>2\*</sup>, LIHONG ZHANG<sup>3\*</sup>, WENYI WU<sup>1</sup>, JIANQING LIN<sup>1</sup>, HAIHONG SHI<sup>1</sup>,  
YIHUANG YU<sup>1</sup>, WEIGANG QIU<sup>1</sup>, JINYAN CHEN<sup>1</sup>, HANSEN DING<sup>1</sup> and XINYAO CHEN<sup>1</sup>

<sup>1</sup>Department of Thyroid and Breast Surgery, The Second Affiliated Clinical School of Medicine, Fujian Medical University;

<sup>2</sup>Department of Endocrinology, No. 910th Hospital of The People's Liberation Army Joint Logistics Support Force;

<sup>3</sup>Department of General Family Medicine, Jinshang Town Health Center, Quanzhou, Fujian 362000, P.R. China

Received October 30, 2023; Accepted February 23, 2024

DOI: 10.3892/ol.2024.14396

**Abstract.** Smad-ubiquitination regulator 2 (SMURF2) functions as a homolog of E6AP carboxyl terminus-type E3 ubiquitin ligase to regulate cell cycle progression and tumor growth factor expression. SMURF2 has been revealed to function as a tumor suppressor in a number of cancers; however, its function in papillary thyroid carcinoma (PTC) remains largely unknown. Therefore, the aim of the present study was to investigate the function of SMURF2 in PTC. Reverse transcription-quantitative PCR and western blotting were used to detect cellular expression of SMURF2 *in vitro*. After increasing or inhibiting the expression of SMURF2, MTT was used to detect the effect on tumor cell proliferation and Transwell assays were used to detect the effect on tumor cell migration and invasion. Finally, ELISA was used to detect the effects on glucose and glutamine metabolism in tumor cells and the findings revealed that SMURF2 was downregulated in PTC tissues. Moreover, SMURF2 inhibited the proliferation, invasion and migration of PTC cells, and promoted their apoptosis. Finally, SMURF2 inhibited cell glycolysis and glutaminolysis and affected metabolism in the PTC cell line, TPC-1. Thus, the findings of the present study suggest that SMURF2 may be a potential target in the treatment of PTC.

## Introduction

The incidence of thyroid cancer recently has increased by 3% in the USA. The primary pathological type is papillary thyroid carcinoma (PTC) (1), with most cases presenting with an indolent clinical course. Furthermore, recurrent or metastatic PTC subsets treated with radioactive iodine ablation, surgery and thyroid-stimulating hormone suppression usually exhibit a favorable prognosis; however, a number of patients with PTC progress to a refractory state, or even succumb to PTC (2). Therefore, identifying molecular factors associated with PTC pathogenesis is essential to developing molecular therapeutics that can inhibit disease progression.

Smad-ubiquitination regulator 2 (SMURF2), a C2-WW-HECT type E3 ubiquitin ligase, is a neural developmental precursor and protein 4 subfamily member that mediates protein degradation via ubiquitination (3). SMURF2 has been demonstrated to exert tumor suppressive effects on normal cells by controlling genome stability (4), whereas it has been shown to inhibit the proliferation of colorectal cancer cells by promoting the ubiquitination of carbohydrate-responsive element binding protein (5). Additionally, SMURF2 was revealed to inhibit the metastasis of hepatocellular carcinoma cells via the ubiquitin-mediated degradation of Smad2 (6). As an E3 ubiquitin ligase, SMURF2 was shown to interfere with the proliferation, migration, and tumorigenesis of colon cancer cells by stimulating the ubiquitination and degradation of special AT-rich sequence-binding protein-1 (SATB1) (7). Thus, SMURF2 has been revealed to be a potent tumor suppressor that limits tumor progression and development; nonetheless, its functions in PTC remain unclear.

Previously, metabolic reprogramming has been identified as a major cancer hallmark (8). Cancer cells reprogram catabolism pathways to generate energy and promote cancer progression and initiation (9). Glutamine and glucose are vital but unusual energy sources for cancer cells (10). Critically, cancer cell metabolism can switch from an oxidative state to a glycolytic state (Warburg effect). Glycolysis and glutaminolysis aid in rapid cancer cell proliferation and promote tumor progression, as well as metabolic reprogramming in PTC (11).

In the present study, the functions of SMURF2 were investigated in PTC. Initially, SMURF2 expression was examined

---

*Correspondence to:* Dr Wenyi Wu, Department of Thyroid and Breast Surgery, The Second Affiliated Clinical School of Medicine, Fujian Medical University, 950 Donghai Street, Quanzhou, Fujian 362000, P.R. China  
E-mail: wwyi8522858@163.com

\*Contributed equally

**Key words:** papillary thyroid carcinoma, Smad-ubiquitination regulator 2, Warburg effect, glutamine metabolism

in PTC cells by western blotting and polymerase chain reaction (PCR). Additionally, SMURF2 expression was interfered with to investigate its effects on major PTC cancer cell processes, including proliferation, migration and invasion. Finally, the effects of SMURF2 on PTC cell metabolism were examined. The findings revealed that altered SMURF2 expression affected aerobic glycolysis, glutamine breakdown, and key PTC cancer cell processes in PTC, indicating its key functions in PTC etiology. Hence, SMURF2 may serve as a novel target for anti-PTC therapies.

## Materials and methods

### *Tissue specimens and cell culture*

**PTC specimens.** A total of 30 pairs of PTC and distant non-tumorous tissues, which were 2 cm away from the cancerous lesions and were confirmed to be tumor-free, were collected from patients treated at the Department of Thyroid and Breast Surgery, The Second Affiliated Clinical School of Medicine, Fujian Medical University (Quanzhou, China) from October 2020 to October 2022. The patients aged 19–68 years (median, 43 years), consisted of 22 women and eight men who were pathologically confirmed as having PTC and staged according to the 2022 World Health Organization Classification of Thyroid Neoplasms criteria (12). No patient received presurgical treatment, such as chemotherapy or radiation therapy. The present study was approved by the Ethics Review Committee of the Second Affiliated Hospital of Fujian Medical University [approval no. 149 (2021)], and all participants provided signed informed consent. Fresh tissue specimens were collected from the surgical room, immediately frozen in liquid nitrogen, and stored at  $-80^{\circ}\text{C}$ . The clinicopathological and follow-up data were obtained from the medical records of the patients.

**Cell culture.** The human TC cell lines, TPC-1 and SW579, were purchased from Guangzhou Ryder Liankang Biotechnology Co., Ltd. and were authenticated by performing short tandem repeat profile analysis. The SW579 cell line was included for comparison and as a reference, and in the future, relevant alternative cell lines will be considered for investigation. The cells were cultured in Roswell Park Memorial Institute (RPMI)-1640 medium supplemented with 5% fetal bovine serum (FBS; cat. no. SH30087.01) and 1% penicillin-streptomycin (cat. no. SH30010; both Hyclone; Cytiva) in a humidified incubator with 5%  $\text{CO}_2$  and 95% air at  $37^{\circ}\text{C}$ .

**Reverse transcription-quantitative PCR (RT-qPCR).** Total cellular RNA was isolated from the cells (TPC-1 and sw579) using TRIzol<sup>®</sup> reagent (Invitrogen; Thermo Fisher Scientific, Inc.) and reverse-transcribed into complementary DNA (cDNA) using an RNase-free DNase I kit (Promega Corporation) per the manufacturer's instructions. The obtained cDNA was subjected to qPCR using 2X SYBR Green qPCR SuperMix (Invitrogen; Thermo Fisher Scientific, Inc.) and a BioPhotometer plus Ebend nucleic acid protein analyzer (Eppendorf). The thermocycling conditions were as follows:  $50^{\circ}\text{C}$  for 2 min,  $95^{\circ}\text{C}$  for 2 min, followed by 40 cycles at  $95^{\circ}\text{C}$  for 15 sec and  $60^{\circ}\text{C}$  for 32 sec. Relative expression was determined using the  $2^{-\Delta\Delta\text{C}_q}$  method (13). Standard manufacturer

amplification protocols were followed using SMURF2 forward, 5'-TTGTTGGACGAATAATGGGA-3' SMURF2 and reverse, 5'-GGATCTACTAAGTCCATGTC-3'; GAPDH forward, 5'-GCTCATTTCAGGGGGGAG-3' and reverse, 5'-GTTGGTGGTGCAGGAGGCA-3' primers.

**Western blotting.** Total cellular protein was extracted with radioimmunoprecipitation assay buffer, and the concentration of the samples was assayed with a bicinchoninic acid protein assay kit (Nanjing KGI Biological Development Co., Ltd.) according to the manufacturer's protocol. Sodium dodecyl sulfate-polyacrylamide gel electrophoresis was performed [Roche Diagnostics (Shanghai) Co., Ltd.] using 10% gel to separate proteins, with 20  $\mu\text{g}$  protein loaded per lane. The proteins were then transferred onto polyvinylidene fluoride membranes (MilliporeSigma). After blocking at room temperature for 1 h in 5% non-fat milk, the membranes were incubated overnight at  $4^{\circ}\text{C}$  with primary antibodies. Subsequently, the membranes were washed with phosphate-buffered saline -0.2% Tween-20 (PBS-T) three times and then incubated with a horseradish peroxidase (HRP)-labeled secondary antibody for 1 h at room temperature ( $37^{\circ}\text{C}$ ). Next, the membranes were lightly washed with PBS-T three times and positive protein signaling was detected using a chemiluminescence detection system (Invigentech). The following primary antibody was used: anti-SMURF2 [EP629Y3] (ab53316; Abcam; 1:1,000). The secondary antibodies used were: Goat anti-rabbit IgG (H+L) and mouse/human ads-HRP (dilution ratio, 1:20,000; cat. no. 4050-05; Southern Biotech). To evaluate the effects of overexpressed SMURF2 on glucose metabolism and glutamine decomposition, western blotting was performed, and key glucose metabolism enzymes, such as lactate dehydrogenase (LDH) and hexokinase 2 (HK2), as well as key glutamine metabolism enzymes, such as alanine/serine/cysteine-prefering transporter 2 (ASCT2) and glutaminase (GLS1), were detected. LDH rabbit monoclonal antibody (mAb; cat. no. 3582; Cell Signaling Technology, Inc.; 1:1,000); recombinant anti-HK II antibody (cat. no. ab209847; Abcam; 1:1,000); recombinant anti-ASCT2 antibody (cat. no. ab237704; Abcam; 1:1,000); anti-GLS1 antibody (cat. no. ab150474; Abcam; 1:500).

**Transfection.** Overexpression plasmids carrying SMURF2 cDNA contain the plasmid backbone of the plasmid plvx-zsgreen-puro (LMAI Bio). The plasmid carried the green fluorescence gene zsgreen, enabling green fluorescence. The SMURF2 small interfering (si)RNA and negative control targeting cDNA sequences were synthesized by Ribobio Co., Ltd. The following siRNA sequences targeting SMURF2 were used: si-NC, 5'-TTCTCCGAACGTGTCACGTTT-3'; si-SMURF2-1 sense, 5'-GAAGTACGCAATGGGAGC GC-3'; si-SMURF2-2 sense, 5'-TGTCAGGCTCTATGTGAA CT-3'; and si-SMURF2-3 sense, 5'-CCACACTTGCTTCAA TCGAA-3'. The antisense sequences of all the siRNAs were as follows: si-NC, 5'-AAGAGGCUUGCACAGUGCAA dTdT-3'; si-SMURF2-1, 5'-CUUGAUGCGUACCCUCG CGdTdT-3'; si-SMURF2-2, 5'-ACAGUCCGAGAUACACU GAdTdT-3'; and si-SMURF2-3, 5'-GGUGUGAACGAAGU AGCUdTdT-3'. These DNA sequences were cloned into the pLKO.1 lentiviral vector (Addgene, Inc.), and the lentiviruses were packaged and produced in 293T cells, after vector

transfection using Lipofectamine® 2000 (cat. no. 11668019; Invitrogen; Thermo Fisher Scientific, Inc.) for 24 h at 37°C and supernatant was collected. The concentration of nucleic acid used was 10 nM and the generation system used was second generation. The lentiviral plasmids used for cell transfection were used at 10 µg in a 10-cm flat cell culture dish and the ratio of lentivirus and packaging and envelope plasmids was 10:8:6, while the transfection was for 48 h at 37°C. The supernatant was then gathered for cell infection. In brief, TPC-1 or SW579 cells were plated into 24-well cell culture plates (5x10<sup>4</sup> cells per well), grown overnight, and then infected with the viral supernatant or control viral particles at MOI of 10 for 48 h at 37°C and analyzed for the efficiency of these siRNAs. siRNA-3 was used for further experiments because it showed the highest interference efficiency. Stably transduced cells were selected using puromycin-containing RPMI-1640. The screening concentration was 12 µg/ml and the maintenance concentration was 4 µg/ml. Transfection was confirmed using a fluorescence microscope (magnification, x200).

**Proliferation assays.** Cells were added to the 96-well plates at a density of 1x10<sup>4</sup> cells/well to verify for cell adhesion. The cells were collected at different time points (0, 24, 48 and 72 h), and examined for proliferation using the Titer 96AQ detection reagent (cat. no. G3582; 1:10; Promega Corp.) after incubating for 4 h at 37°C. The absorbance was measured using a microplate reader (Multiscan MK3; Thermo Fisher Scientific, Inc.) at 490 nm, followed by 3-(4,5-dimethylthiazol-2-yl)-2,5-diphenyl-2H-tetrazolium bromide (MTT) assay. The solvent used to dissolve the purple formazan was dimethyl sulfoxide. A wavelength of 490 nm was used to measure formazan.

**Transwell assays.** Transwell chambers were purchased from Corning, Inc. to assess the migration and invasion abilities of PTC cells. The cells were resuspended in the RPMI-1640 medium containing 10% FBS at 1x10<sup>5</sup> cells/ml. Matrigel (Corning, Inc.) was added to the upper chambers, and, when the gel was set, 100 µl of cell suspensions were added to each well and cultured for 48 h at 37°C. The lower chambers contained the RPMI-1640 medium with 20% FBS (Invitrogen; Thermo Fisher Scientific, Inc.). Subsequently, cells that remained on the filter surface were removed using a cotton swab, whereas cells that invaded the gel were first fixed in 4% paraformaldehyde, then fixed in 10% methanol, stained with 0.1% crystal violet for 10 min at room temperature, and visualized using an inverted fluorescence microscope (Olympus CKX41; Olympus Corp.). The number of invasive cells in five random fields (magnification, x400) was counted and averaged. For migration studies, the cells were added to the upper chambers without Matrigel, and the rest of the steps were the same as for invasion studies. The assay was performed in duplicate and repeated three times.

**ELISA.** All of the following experimental samples were obtained from cultured *in vitro* thyroid cells. Lactate, ATP, glutamate, α-ketoglutarate and glutamine levels, as well as glucose consumption were evaluated using ELISA after overexpression of SMURF2. ELISA kits included lactate (cat. no. WK-SU62; Shanghai Valan Biotechnology Co., Ltd.),

ATP (cat. no. LE-H3380; Hefei Laier Biotechnology Co., Ltd.), glucose consumption (cat. no. Keshun-0017; Shanghai Keshun Biotechnology Co., Ltd.), glutamate (cat. no. 140739; Nanjing Senbeiga Biotechnology Co., Ltd.), α-ketoglutarate (cat. no. XGE64578; Shanghai Sig Biotechnology Co., Ltd.) and glutamine (cat. no. KL-Gln-Hu; Shanghai Kanglang Biotechnology Co., Ltd.). The relevant experiments were performed according to the protocols provided in the kits. ELISA was performed in duplicate and repeated at least twice.

**Statistical analysis.** SPSS 27 software (IBM Corp.) was used for statistical analysis. The experiments were performed in triplicate independently and the resultant data are summarized as the mean ± SD. The paired sample t-test was used for the comparison of clinical paired sample differences, the independent sample t-test was used for the difference in mean between the two groups, and one-way ANOVA analysis was used to compare the difference in mean between three or more groups. When performing multiple comparisons, the Tukey-Kramer post hoc test was used. P<0.05 and P<0.01 were considered to indicate statistically significant differences.

## Results

**SMURF2 is downregulated in PTC tissues.** To investigate SMURF2 expression in PTC, RT-qPCR was performed and SMURF2 mRNA levels were examined in PTC and normal adjacent tissues (n=30 each). SMURF2 mRNA levels were significantly lower in the PTC tissues compared with the healthy adjacent tissues (Fig. 1A). Similarly, western blotting showed that SMURF2 levels were lower in the PTC tissues compared with the healthy adjacent tissues (Fig. 1B). Clinical data from the patients with PTC were examined to determine associations between SMURF2 mRNA expression and clinicopathological characteristics, revealing that SMURF2 mRNA expression was associated with lymph node metastasis, but not with age, sex, tumor size, number of lesions or extrathyroidal extension (Table I).

**SMURF2 affects key PTC cancer phenotypes.** The function of SMURF2 was determined by silencing the protein using si-SMURF2-1, si-SMURF2-2 or si-SMURF2-3, and si-NC was used as a negative control. *In vitro*, SMURF2 silencing efficiency in the cell lines, TPC-1 and SW579, was assessed using RT-qPCR. The results revealed that SMURF2 expression was significantly decreased with transfection of si-SMURF2-3 compared with si-NC expression in TPC-1 cells and these cells were selected for subsequent experiments (Fig. 2A, B and F). Subsequently, the cell lines were assigned to five groups as follows: Untreated cells, si-NC, si-SMURF2, SMURF2 overexpression (ov-SMURF2), and overexpression control (ov-NC) to assess the effect of SMURF2 on malignant biological function in tumor cells, respectively. Cell proliferation was examined using MTT assays. Compared with untreated cells and overexpression control (ov-NC), ov-SMURF2 markedly decreased cell proliferation (Fig. 2C). Moreover, compared with untreated cells and overexpression control (ov-NC), the ov-SMURF2 cell lines showed markedly reduced migration and invasion abilities using Transwell assays (Fig. 2D and E). Thus, SMURF2 expression was downregulated in PTC cells,

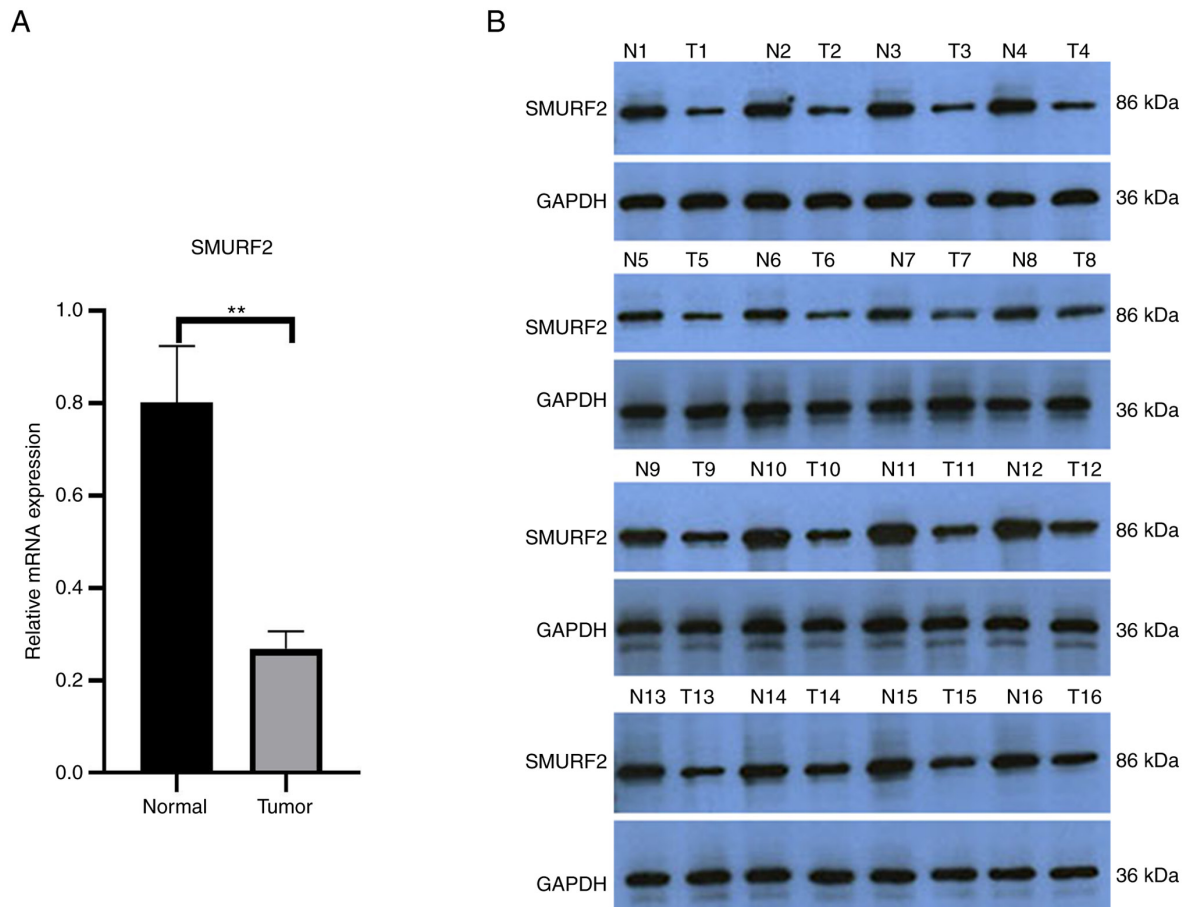


Figure 1. SMURF2 levels are reduced in PTC tissues and found to be associated with lymphatic metastasis. (A) The histogram shows the relative SMURF2 mRNA levels in PTC (n=30) and normal adjacent tissues (n=30). (B) Western blotting determined the SMURF2 protein levels in PTC (n=30) and normal adjacent tissues (n=30). \*\*P<0.01. SMURF2, Smad-ubiquitination regulator 2; PTC, papillary thyroid carcinoma; N, normal; T, tumor.

Table I. Association of SMURF2 mRNA level with clinical features.

Variable	No. of patients	SMURF2 (mRNA)	T-value	P-value
Sex				
Female	22	0.27±0.00	-0.583	0.565
Male	8	0.27±0.11		
Patient age at diagnosis				
≤45	18	0.28±0.42	0.592	0.558
>45	12	0.27±0.28		
Tumor size (cm)				
<2	12	0.27±0.01	-0.393	0.697
≥2	18	0.28±0.00		
N stage (AJCC)				
N0 and Nx	13	0.29±0.00	2.614	0.014
N1	17	0.26±0.00		
Gland outside invasion				
No	23	0.27±0.00	-0.475	0.638
Yes	7	0.28±0.13		
Tumor location				
One lobe	24	0.27±0.00	-0.483	0.633
More than one lobe	6	0.28±0.01		

SMURF2, Smad-ubiquitination regulator 2; AJCC, American Joint Committee on Cancer.



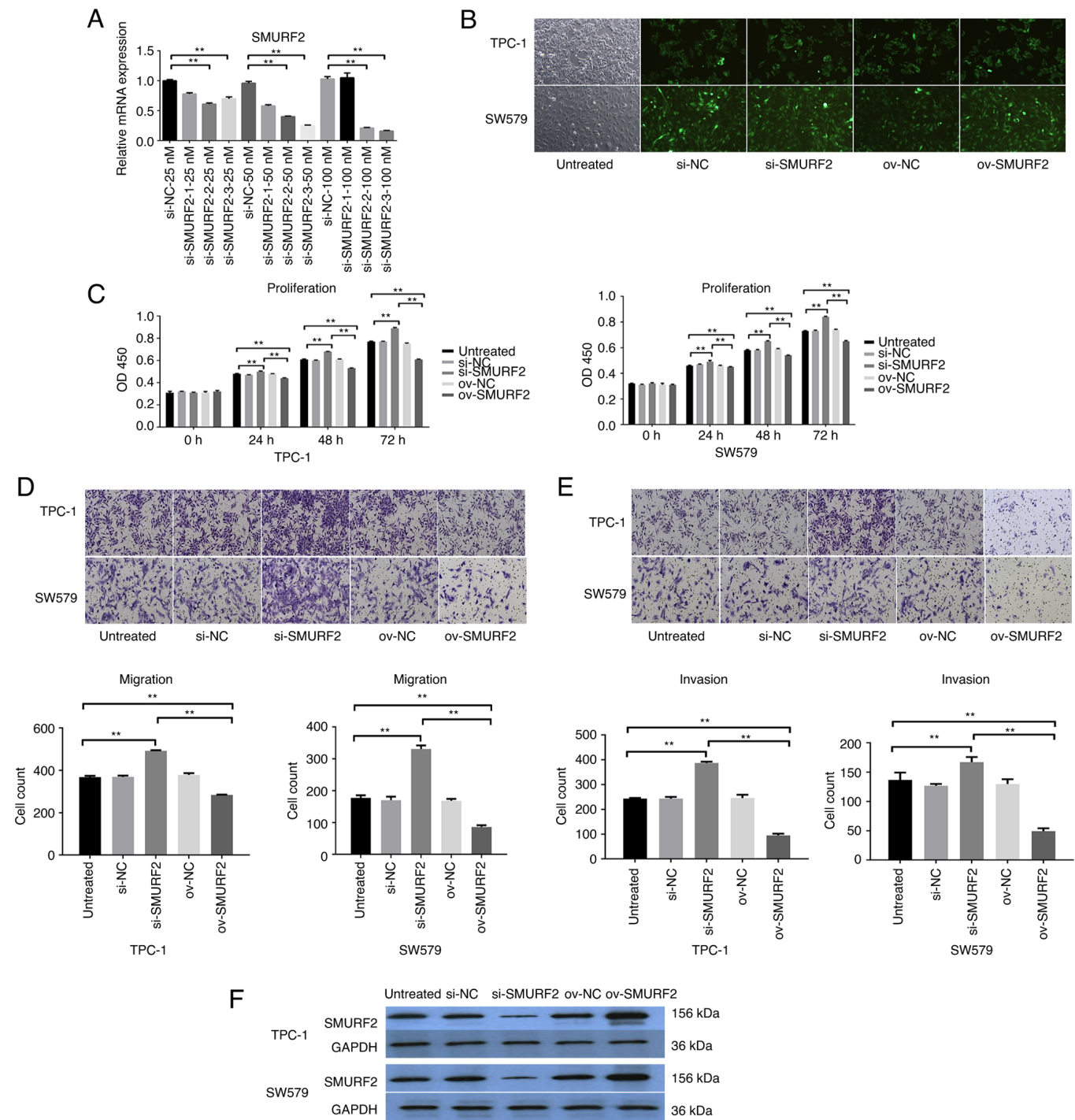


Figure 2. SMURF2 affects key papillary thyroid carcinoma cell phenotypes. (A) SMURF2 interference efficiency. TPC-1 cells were grown and infected with SMURF2 siRNAs for 48 h and subjected to reverse transcription-quantitative PCR analysis of SMURF2 expression to test the interference efficiency of SMURF2 siRNAs. (B) Viral transfection images. (C) The 3-(4,5-dimethylthiazol-2-yl)-2,5-diphenyl-2H-tetrazolium bromide assay was performed to examine the effects of SMURF2 stable overexpression or silencing on cell proliferation. (D) Transwell assays were performed to assess the effects of SMURF2 stable overexpression or silencing on cell migration. (E) SMURF2 overexpression or silencing effects on cell invasion using Transwell assays. \*\*P<0.01. (F) TPC-1 and SW579 cells with stable SMURF2 knockdown or overexpression underwent western blot analysis of SMURF2 protein expression. Magnification x200 for B, D, and E. SMURF2, Smad-ubiquitination regulator 2; si-, small interfering RNA; NC, negative control; ov, overexpressed.

whereas its overexpression inhibited key PTC cancer cell processes.

*SMURF2 inhibits the Warburg effect in PTC cells.* The Warburg effect is an anaerobic glycolysis phenomenon; unlike normal cells, which use oxygen, tumor cells undergo anaerobic fermentation to meet their energy need, irrespective

of the aerobic environment (14). To further understand SMURF2 function in PTC, lactate, LDH, HK2 and ATP levels, as well as glucose consumption in TPC-1 cells were examined. Compared with empty-vector control cells, the SMURF2 overexpressing cells showed decreased lactate. Conversely, SMURF2 silencing increased lactate in the cell lines (Fig. 3A). Compared with the untreated group and

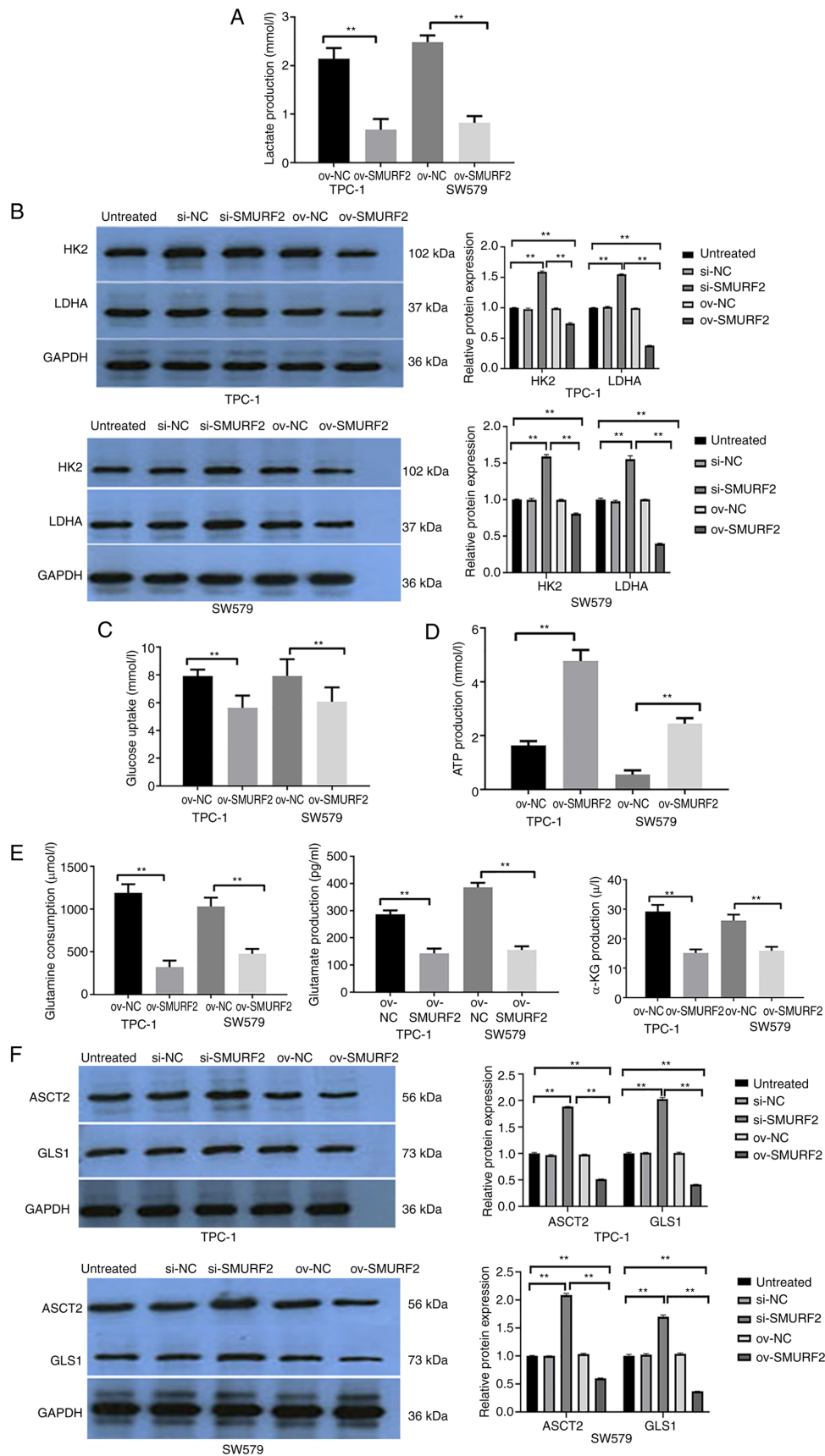


Figure 3. SMURF2 inhibits the Warburg effect and glutamine catabolism in papillary thyroid carcinoma. (A) Lactate production in empty vector control cells, and PTC-1 and SW579 cells stably overexpressing SMURF2. (B) LDH and HK2 activities in cells stably overexpressing SMURF2 and empty vector control cells. (C) Glucose uptake in cells stably overexpressing SMURF2 and empty vector control cells. (D) ATP content was determined in cells stably overexpressing SMURF2 and empty vector control cells. (E) Glutamine consumption, as well as glutamate and  $\alpha$ -KG production in cells overexpressing SMURF2. (F) The key glutaminase enzymes ASCT2 and GLS1 in empty vector cells, and cells stably overexpressing SMURF2. \*\* $P < 0.01$ . SMURF2, Smad-ubiquitination regulator 2; LDH, lactate dehydrogenase; HK2, hexokinase 2;  $\alpha$ -KG,  $\alpha$ -ketoglutarate; ASCT2, alanine/serine/cysteine-preferred transporter 2; GLS1, glutaminase; ov, overexpressed; NC, negative control; si-, small interfering RNA.

si-NC group, the protein activities of LDHA and HK2 in the si-SMURF2 group were significantly enhanced. By contrast, compared with the untreated group and the ov-NC group, the protein activities of LDHA and HK2 in the ov-SMURF2 group were significantly weakened (Fig. 3B). Furthermore, compared with the empty vector control cells, cell lines over-expressing SMURF2 showed higher ATP and lower glucose consumption levels. Conversely, SMURF2 silencing led to the opposite effects (Fig. 3C and D). Therefore, SMURF2 exerted inhibitory effects on glycolysis in PTC cells.

**SMURF2 affects glutamine metabolism in PTC cells.** In cancer, glutamine catabolism is a characteristic metabolic pattern observed after metabolic reprogramming (15). To further understand the mechanism of action of SMURF2, glutamine consumption, glutamate and  $\alpha$ -ketoglutarate production, as well as ASCT2 and GLS1 enzyme activities in the SMURF2 overexpressing cells were analyzed. Compared with untreated cells and overexpression control (ov-NC), the SMURF2 overexpressing cells exhibited significantly decreased glutamine consumption, and glutamate and  $\alpha$ -ketoglutarate production (Fig. 3E). Furthermore, decreased ASCT2 and GLS1 levels were observed in TPC-1 and SW579 cells (Fig. 3F). Thus, SMURF2 inhibited glutamine catabolism in PTC cells.

## Discussion

Ubiquitination is a common ATP-dependent cascade that occurs in eukaryotes (16) and requires at least the following three enzymes: Ubiquitin-conjugating enzyme E2, ubiquitin-activating enzyme E1, and ubiquitin ligase E3 (15). Ubiquitin ligase E3 is critical, as it targets and degrades substrates via the ubiquitin-proteasome system (17). SMURF2, an E3 ubiquitin ligase, exhibits key functions in malignant tumors, such as preventing colorectal cancer progression by ubiquitinating the YY1 protein and decreasing its stability (18). Additionally, upstream stimulatory factor 2 was revealed to affect breast malignancy development by inhibiting SMURF2 transcription (19). Furthermore, SMURF2 transcription inhibition enhanced chemoradiotherapy efficacy in non-small cell lung cancer (20). In the present study, it was revealed that SMURF2 expression in PTC tissues was downregulated. Thus, SMURF2 may act as a tumor suppressor in PTC cells.

To further confirm the role of SMURF2 in PTC, the effect of SMURF2 alterations on PTC cell functions and the metabolism was investigated in TPC-1 cells. SMURF2 silencing promoted key TPC-1 malignant phenotypes. Furthermore, it inhibited glucose and glutamine metabolism in TPC-1 cells, which would affect tumor progression and clinical prognosis in PTC. The underlying mechanism of SMURF2 glucose and glutamine metabolism inhibition in TPC-1 cells will be examined in future studies. Current data suggest that SMURF2 inhibits glycometabolism and glutamine metabolism in cancer cells. However, the current data warrants confirmation via *in vivo* and clinical studies. It is therefore important to explore how SMURF2 regulates its downstream factors in controlling the progression of PTC. Despite its numerous strengths, there are some limitations

to this study. For example, the present study revealed that SMURF2 inhibits the malignant biological behavior and metabolism of PTC, however the relationship between tumor stage and gene expression as well as the results of enhanced immunohistochemistry will be further explored and improved in future studies. In addition, the mechanism of the effect of SMURF2 was not determined. Further studies are therefore required to determine the underlying regulatory mechanism. In conclusion, in PTC clinical specimens, SMURF2 expression was low. *In vitro*, SMURF2 inhibited the malignant phenotype of PTC cells, which could affect the clinical prognosis of PTC by mediating metabolic reprogramming of TPC-1 cells. Therefore, SMURF2 may be a potential therapeutic target for the treatment of PTC.

## Acknowledgements

Not applicable.

## Funding

The present study was partially supported by a grant from the Fujian Provincial Natural Science Foundation (grant no. 2021J01251), the Medjaden Academy and Research Foundation for Young Scientists (grant no. MJA2306089) and the Key Clinical Specialty Discipline Construction Program of Fujian, P.R.C (Fujian Health Medicine and Politics [2022]884).

## Availability of data and materials

The data generated in the present study are included in the figures and/or tables of this article.

## Authors' contributions

GL, WW and LitZ conducted the experiments. JL and HS analyzed the results. GL and LihZ prepared and revised the manuscript. LihZ made significant contributions to data analysis and interpretation. LitZ, YY and WQ designed the present study. YY and WQ revised and discussed the manuscript. JC, HD and XC made substantial contributions to interpretation of data. GL and WW confirm the authenticity of all the raw data. All authors read and approved the final version of the manuscript.

## Ethics approval and consent to participate

The present study was approved by the Ethics Review Committee of the Second Affiliated Hospital of Fujian Medical University [approval no. 149 (2021)], and all participants provided signed informed consent.

## Patient consent for publication

Not applicable.

## Competing interests

The authors declare that they have no competing interests.

## References

1. Lim H, Devesa SS, Sosa JA, Check D and Kitahara CM: Trends in thyroid cancer incidence and mortality in the united states, 1974-2013. *JAMA* 317: 1338-1348, 2017.
2. Pu WL, Shi X, Yu PC, Zhang MY, Liu ZY, Tan L, Han P, Wang Y, Ji D, Gan H, *et al*: Single-cell transcriptomic analysis of the tumor ecosystems underlying initiation and progression of papillary thyroid carcinoma. *Nat Commun* 12: 6058, 2021.
3. Ilic N, Tao YL, Boutros-Suleiman S, Kadali VN, Emanuelli A, Levy-Cohen G and Blank M: SMURF2-mediated ubiquitin signaling plays an essential role in the regulation of PARP1 PARYlating activity, molecular interactions, and functions in mammalian cells. *FASEB J* 35: e21436, 2021.
4. Blank M, Tang Y, Yamashita M, Burkett SS, Cheng SY and Zhang YE: A tumor suppressor function of Smurf2 associated with controlling chromatin landscape and genome stability through RNF20. *Nat Med* 18: 227-234, 2012.
5. Li YK, Yang DQ, Tian N, Zhang P, Zhu YM, Meng J, Feng M, Lu Y, Liu Q, Tong L, *et al*: The ubiquitination ligase SMURF2 reduces aerobic glycolysis and colorectal cancer cell proliferation by promoting ChREBP ubiquitination and degradation. *J Biol Chem* 294: 14745-14756, 2019.
6. Song DQ, Li SY, Ning LX, Zhang SC and Cai Y: Smurf2 suppresses the metastasis of hepatocellular carcinoma via ubiquitin degradation of Smad2. *Open Med (Wars)* 17: 384-396, 2022.
7. Yu L, Dong L, Wang Y, Liu L, Long H, Li H, Li J, Yang X, Liu Z, Duan G, *et al*: Reversible regulation of SATB1 ubiquitination by USP47 and SMURF2 mediates colon cancer cell proliferation and tumor progression. *Cancer Lett* 448: 40-51, 2019.
8. Li Z and Zhang H: Reprogramming of glucose, fatty acid and amino acid metabolism for cancer progression. *Biochim Biophys Acta Rev Cancer* 73: 377-392, 2016.
9. Sun LC, Suo CX, Li ST, Zhang HF and Gao P: Metabolic reprogramming for cancer cells and their microenvironment: Beyond the Warburg Effect. *Biochim Biophys Acta Rev Cancer* 1870: 51-66, 2018.
10. Liu Y, Zhou Q, Song SL and Tang S: Integrating metabolic reprogramming and metabolic imaging to predict breast cancer therapeutic responses. *Trends Endocrinol Metab* 32: 762-775, 2021.
11. Coelho RG, Fortunato RS and Carvalho DP: Metabolic reprogramming in thyroid carcinoma. *Front Oncol* 8: 82, 2018.
12. Cameselle-Teijeiro JM: Changes and perspectives in the New 2022 WHO classification of thyroid neoplasms. *Rev Esp Patol* 55: 145-148, 2022 (In Spanish).
13. Livak KJ and Schmittgen TD: Analysis of relative gene expression data using real-time quantitative PCR and the 2(-Delta Delta C(T)) method. *Methods* 25: 402-408, 2001.
14. Sun T, Liu Z and Yang Q: The role of ubiquitination and deubiquitination in cancer metabolism. *Mol Cancer* 19: 146, 2020.
15. Bedford L, Lowe J, Dick LR, Mayer RJ and Brownell JE: Ubiquitin-like protein conjugation and the ubiquitin-proteasome system as drug targets. *Nat Rev Drug Discov* 10: 29-46, 2011.
16. Sun TS, Liu ZN and Yang Q: The role of ubiquitination and deubiquitination in cancer metabolism. *Mol Cancer* 19: 146, 2020.
17. Fan Q, Wang Q, Cai RJ, Yuan HH and Xu M: The ubiquitin system: Orchestrating cellular signals in non-small-cell lung cancer. *Cell Mol Biol Lett* 25: 1, 2020.
18. Gao QF, Wang SC and Zhang ZY: E3 ubiquitin ligase SMURF2 prevents colorectal cancer by reducing the stability of the YY1 protein and inhibiting the SENP1/c-myc axis. *Gene Ther* 30: 51-63, 2023.
19. Tan YW, Chen YJ, Du MG, Peng ZQ and Xie P: USF2 inhibits the transcriptional activity of Smurf1 and Smurf2 to promote breast cancer tumorigenesis. *Cell Signal* 53: 49-58, 2019.
20. Chaudhary KR, Kinslow CJ, Cheng HY, Silva JM, Yu JY, Wang TJ, Hei TK, Halmos B and Cheng SK: Smurf2 inhibition enhances chemotherapy and radiation sensitivity in non-small-cell lung cancer. *Sci Rep* 12: 10140, 2022.